

Short-term phytotoxicity in *Brassica napus* (L.) in response to pre-emergently applied metazachlor: A microcosm study

Peer-reviewed author version

VERCAMPT, Hanne; Koleva, Lyubka; Vassilev, Andon; VANGRONSVELD, Jaco & CUYPERS, Ann (2017) Short-term phytotoxicity in *Brassica napus* (L.) in response to pre-emergently applied metazachlor: A microcosm study. In: ENVIRONMENTAL TOXICOLOGY AND CHEMISTRY, 36(1), p. 59-70.

DOI: 10.1002/etc.3538

Handle: <http://hdl.handle.net/1942/23281>

1
2
3
4
5
6
7
8

Running head:

Short-term phytotoxic effects of metazachlor on oilseed rape

Corresponding author:

Cuypers Ann

Agoralaan Building D, 3590 Diepenbeek, Belgium

Tel +32 11 268326

E-mail ann.cuypers@uhasselt.be

9

Title:

10 **Short-term phytotoxicity in *Brassica napus* (L.) in response to pre-emergently applied**
11 **metazachlor: a microcosm study**

12

13 Vercampt Hanne[†], Koleva Lyubka[‡], Vassilev Andon[‡], Vangronsveld Jaco[†] and Cuypers

14

Ann^{†*}

15

16 [†]Hasselt University, Centre for Environmental Sciences, Agoralaan Building D, 3590

17

Diepenbeek, Belgium

18

[‡]Agricultural University of Plovdiv, Department of Plant Physiology and Biochemistry,

19

Plovdiv, Bulgaria

20

*Corresponding author: **E-mail** ann.cuypers@uhasselt.be **Tel** +32 11 268326

21
22
23
24
25
26
27
28
29
30
31
32
33
34
35
36
37
38
39
40
41

ABSTRACT

In accordance with realistic application approaches, a short-term one-factorial experiment was set up to investigate the phytotoxic impact of pre-emergent application of the chloroacetamide herbicide metazachlor on *Brassica napus*. In addition to morphological parameters, the underlying processes that ultimately determine the extent of herbicide-induced phytotoxicity, *i.e.* herbicide metabolisation and cellular antioxidant defence, were examined. The present study demonstrated that metazachlor provoked fasciation of the leaves closely after emergence, which could possibly be addressed to its working mechanism whereby cell division is impaired through the inhibition of very long chain fatty acid synthesis. The increased activities of antioxidative enzymes and metabolites in leaf tissue indicated the presence of reactive oxygen species under the influence of metazachlor. This resulted in oxidative damage in the form of membrane lipid peroxidation. Simultaneously, the increased activity of glutathione-S-transferase (GST) and the shift in glutathione (GSH) redox state suggested the activation of the detoxification metabolism. This occurred however at the expense of growth, with a temporary reduction in plant height and weight after application. The results indicated that metazachlor disappeared within 3 to 4 months after application, which resulted in the recovery of the crop. In conclusion, metazachlor induces phytotoxicity in the short-term, either directly through its mode of action or indirectly through the induction of oxidative stress, which resulted in a temporary reduction in growth.

Key words: *Brassica napus*, metazachlor, phytotoxicity, stress response, toxic effects

INTRODUCTION

42

43 Metazachlor is a pre-emergently used herbicide in the cultivation of the oilseed crop,
44 *Brassica napus*, to chemically prevent the settling and growth of broadleaved weeds and
45 annual grasses. As a chloroacetamide, metazachlor is known for inhibiting lipid biosynthesis
46 and hence the formation of very long chain fatty acids (VLCFA) [1]. Like most herbicides,
47 metazachlor can affect other non-target species via soil infiltration, drainage and run-off [2,3].
48 Even before it enters the ecosystem, the herbicidal compound can potentially affect the
49 cultivated crop. This can subsequently result in reductions in yield [4], morphological
50 aberrations [5], induction of oxidative stress [6], increased lipid peroxidation of membranes
51 [7] and decreased chlorophyll content [8]. Results derived from field experiments are often
52 subject to large variations between plots from a certain condition, resulting in a lack of
53 statistical support. This is due to the fact that field experiments cannot exclude the complex
54 interaction of external factors, such as direction and rate of drainage, the presence of
55 herbivores (*e.g.* snails), heterogeneity of the soil, etc. This microcosm study aims to exclude
56 these side effects by the use of a one-factorial experimental set-up.

57 The occurrence and extent of phytotoxicity of metazachlor in *B. napus* are determined
58 either by the crop's capacity to detoxify the herbicide or its capacity to cope with
59 metazachlor-induced oxidative stress. The detoxification metabolism of a crop plays an
60 important role in the tolerance of a crop against herbicides, with a significant role for
61 glutathione-S-transferase (GST) [9,10]. Once herbicidal compounds are present in the cell
62 cytoplasm the structure and reactivity of the compound will be modified by cytochrome P450
63 proteins in the first phase of detoxification. In the second phase, the modified herbicidal
64 compound is conjugated with glutathione (GSH) by the action of GSTs. In the third phase of
65 herbicide detoxification, GSH will function as a tag for the compartmentalization of the
66 herbicidal compound into either the vacuole or the cell membrane. Herbicidal compounds are

67 known to induce the activity of GST in most crops species [6,11,12]. Based on their sequence
68 identity, gene organisation and active site residues, plant GST's can be divided into 5 classes;
69 tau, phi, theta, zeta and lambda [13]. Tau and phi class GSTs are plant-specific and do not
70 occur in mammalian species like all other plant GST classes. GST isoenzymes that belong to
71 the same class have a 40 to 60 % identity in their primary structure. Structurally, GSTs are
72 composed of 2 subunits that can be either identical (homodimeric) or distinct (heterodimeric).
73 Each subunit contains a kinetically independent active site with distinct domains for the GSH
74 (G-site) and the electrophilic substrate (H-site). With each subunit encoded by a separate
75 gene, plants contain complex multigene families of GSTs. Hence, the various subunits may be
76 able to dimerise in many permutations, producing multiple homo- and hetero-dimeric GST
77 isoenzymes [14]. The GST isoenzymes involved in xenobiotic metabolism are subjected to
78 discrete regulation, showing distinct but overlapping substrate specificities. From
79 complementation studies, it is likely that quite dissimilar GSTs share similar functions [15].
80 Despite the association between GSTs and plant stress responses, it remains unclear whether
81 different GST classes are substrate specific. The inducibility of phi and tau class GSTs after
82 plant exposure to either biotic or abiotic stresses is a characteristic feature of these genes [16].
83 Several tau class GSTs are known to be strongly induced during cell division [16]. Phi class
84 GSTs have been shown to be highly reactive towards chloroacetamide and thiocarbamate
85 herbicides [11,17].

86 Initially after herbicide application, when detoxification is either activated or at its full
87 turnover, the non-detoxified fraction of cytosolic herbicidal compounds can indirectly cause
88 oxidative damage at different cellular levels by the induction of oxidative stress. Herbicide-
89 induced oxidative stress has been described in crops [18,19] and for chloroacetamides, such
90 as alachlor and metolachlor, in particular [20,21]. Herbicides from different classes of mode
91 of action can negatively affect crop morphology [22] and physiology, ranging from

92 destabilisation of cellular membranes [23] to pigment profiles [24]. However, the underlying
93 mechanisms of phytotoxicity are not well addressed in literature. Due to the relatively short
94 degradation rate of metazachlor, which ranges between 3 to 4 months, it is important to
95 monitor metazachlor-induced phytotoxicity closely after application in this short-term
96 microcosm study. A one-factorial microcosm experiment was set up to monitor (i) growth,
97 development and herbicide uptake of the crop *B. napus* during 9 weeks after treatment with
98 metazachlor and (ii) to monitor cellular structure, such as membrane integrity, pigment and
99 nutrient content, and cell functioning, such as herbicide detoxification and antioxidant
100 defence mechanism, of *B. napus* within 2 and 4 weeks after pre-emergent application of
101 metazachlor.

MATERIALS AND METHODS

102
103
104
105
106
107
108
109
110
111
112
113
114
115
116
117
118
119
120
121
122
123
124
125
126

Experimental design and methodology

Three days before sowing, *B. napus* (cultivar *Remy*) seeds were surface sterilised. Hereby, seeds were washed in a 0.1 % sodium hypochlorite solution for 2 min and subsequently rinsed thoroughly with deionised water. Next, seeds were rinsed in deionised water for 20 min and then stored in a closed Petri dish on a moistened filter. After being incubated in the dark at 4 °C during 2 nights, seeds were separately sown in microcosms on 1.3 kg sandy soil at approximately 1 cm depth. In each microcosm 6 seeds were sown. The day after sowing, 10 mL of metazachlor solution was applied on the soil surface in the following concentrations; 0 mM, 0.2 mM and 0.4 mM metazachlor, which corresponded with 0 mg, 0.5 mg and 1 mg active ingredient per microcosm. Every 2 days, 10 to 50 mL $\frac{1}{2}$ Hoagland nutrient solution was supplied. Plants were grown in a growth chamber under controlled environmental conditions set at a 12 h photoperiod, 65 % relative humidity and day/night temperatures of 22 °C and 18 °C, respectively. A combination of blue, red and far-red LED modules simulated the photosynthetic active radiation (PAR) of 200 $\mu\text{mol}/\text{m}^2\text{s}$ of sunlight. Germination was determined by counting the percentage of seeds emerged within 7 days after metazachlor application. Thereafter, the amount of plants was reduced to 1 plant per microcosm. Growth was monitored daily during 7 weeks by determining the growth stage of each individual plant according to Lancashire [et al.](#) [25]. Metazachlor uptake into the aboveground plant parts was monitored 14, 28 and 42 days after treatment (DAT). Leaf tissue for biochemical analyses was collected 14 and 28 DAT, snap frozen in liquid nitrogen and subsequently stored at -70 °C. During sampling, weight, root and shoot length were measured. In addition to these time points, fresh weight was recorded at 9 weeks after treatment (63 DAT).

127 *Lipid peroxidation*

128 Lipid peroxidation of cell membranes was determined by the measurement of
129 thiobarbituric acid (TBA) reactive metabolites [26]. Fresh leaf tissue (100 mg) was
130 homogenised in 0.1 % trichloroacetic acid (TCA). After 30 min of incubation with 0.5 %
131 TBA in 20 % TCA at 95 °C, the extract was cooled for 5 min on ice (4 °C) and subsequently
132 centrifuged for 10 min at 20.000 g (4 °C). The absorbance of the supernatant was measured at
133 532 nm and corrected for unspecific binding at 600 nm.

134

135 *Pigment profile*

136 Chlorophyll *a*, chlorophyll *b* and carotenoid concentrations were determined according to
137 Lichtenthaler [et al.](#) [27]. Fresh leaf material (100 mg) was homogenised in 80 % acetone in
138 cooled mortars, in darkness. After centrifugation (9.000 g, 5 min), the volume of the
139 supernatant was determined and subsequently 10 times diluted in 80 % acetone. The leaf
140 extract was measured spectrophotometrically at 663 nm, 646 nm and 470 nm, and
141 subsequently the pigment profile was calculated.

142

143 *Potassium leakage*

144 Potassium leakage was monitored as a measure for cell membrane stability. After cutting a
145 leaf, the surface of the leaf was washed with Milli-Q water, dried and subsequently cut in 2
146 halves. Thereby, the main leaf nerve was removed. After weighing each half of the leaf, one
147 part was incubated in 10 mL of Milli-Q water at 4°C during 3 hours and the other part was
148 incubated in 10 mL of Milli-Q water at 95°C during 3 hours. The concentration of potassium
149 was determined in both extracts by ICP-OES and represented the extracellular and the total
150 concentration of potassium present in the leaf, respectively.

151

152 *H₂O₂ quantification*

153 The presence of H₂O₂ in the first leaf pair was determined by qualitative 3,3'-
154 diaminobenzidine (DAB) staining [28]. As DAB precipitates as a brown complex after being
155 oxidised by H₂O₂, the latter could be located visually. Leaves were carefully cut at their basis,
156 put in the dark and immediately vacuum infiltrated with DAB in 10 mM Na₂HPO₄ buffer
157 (pH 3) for 5 min. Subsequently the samples were shaken for 4 h at 80 rpm in dark conditions.
158 After being bleached for 15 min in ethanol:acetic acid:glycerol (3:1:1) at 95 °C, leaves were
159 stored in acetic acid (20 %) at 4 °C before being monitored. The following day, detailed
160 close-up pictures were taken from each separate leaf using a binocular microscope, a digital
161 camera and BTV-pro software (Bensoftware).

162

163 *Total antioxidant capacity*

164 The ferric reducing antioxidant capacity (FRAP) assay was used to determine the capacity
165 of lipophilic and hydrophilic antioxidant fractions [29]. Fresh leaf tissue (100 mg) was
166 homogenised in 0.01 N Na-EDTA. After centrifugation (30 min, 15.000 g, 4 °C), the
167 hydrophilic fraction was located in the supernatant. The lipophilic fraction, which was located
168 in the pellet, was further extracted in 80 % acetone before analysis. Freshly prepared FRAP
169 reagent, containing 100 mM 2,4,6-Tris(2-pyridyl)-s-triazine (TPTZ) and 200 mM FeCl₃ in
170 sodium acetic buffer (pH 3.6-4), was added to both fractions. The measurement of the anti-
171 oxidative capacity of the sample was based on its ability to reduce the yellow-coloured Fe³⁺-
172 TPTZ complex to the blue-coloured ferrous form, which was spectrophotometrically recorded
173 at 593 nm. The results were calculated by standard curves prepared with known
174 concentrations of Trolox and were expressed as μmol Trolox equivalents/g FW.

175

176

177 *Antioxidant enzyme activities*

178 Proteins were extracted from leaf samples by a 2-step ammonium sulphate precipitation
179 method. All steps were performed at 4 °C. Leaf material was incubated for 30 min in fresh
180 0.1 M Tris/HCl buffer (pH 7.8), containing 5 mM EDTA, 5 mM DTE, 1% PVP and 1 %
181 Nondidet. After 30 min of centrifugation (50.000 g), the supernatant was incubated for 30 min
182 with 40 % (NH₄)₂ SO₄. After a second round of centrifugation, the supernatant was incubated
183 for 30 min with 80 % (NH₄)₂ SO₄. The extract was subsequently desalted by running over
184 PD 10 columns (2 min, 950 g, 4 °C) and directly stored at -80 °C for further analysis of
185 enzyme activities. All enzyme activities were determined at 25 °C in 1 mL cuvettes. Eight
186 biological replicates were used from each condition.

187 *Superoxide dismutase (SOD)* activity was determined in 33 mM KH₂PO₄ reaction buffer (pH
188 7.8) and 0.1 mM EDTA [30]. By adding 60 mU xanthine oxidase to 0.05 mM xanthine, uric
189 acid is formed. In this reaction, superoxide is formed as a by-product and reduces cytochrome
190 C (0.01 mM) in a blank sample. By adding plant extract, SOD activity is calculated indirectly
191 by measuring the inhibition of formation of reduced cytochrome C at 550 nm. The amount of
192 SOD inhibiting the production of reduced Cyt C with 50 % is defined as 1 unit of SOD
193 activity.

194 *Catalase (CAT)* activity was determined in 75 mM KH₂PO₄ reaction buffer (pH 7) [31]. After
195 addition of 1 mM H₂O₂, catalase activity is calculated by the rate at which H₂O₂ is reduced to
196 H₂O and O₂ and hence by measuring the decrease of H₂O₂ spectrophotometrically at 240 nm.

197 *Glutathione reductase (GR)* was determined in 1 mM Tris and 1 mM EDTA reaction buffer
198 (pH 8) [31]. By adding 1.5 mM glutathione disulfide (GSSG) and 0.1 mM NADPH to the
199 reaction buffer, GR present in the leaf extract catalyses the reduction of GSSG to GSH,
200 through simultaneous consumption of NADPH. Measuring the oxidation of NADPH at
201 340 nm makes it possible to calculate the GR activity.

202 *Guaiacol peroxidase (GPx)* was determined in 75 mM KH_2PO_4 reaction buffer (pH 7) [31].
203 Adding 1 mM H_2O_2 and 2 mM guaiacol to the reaction buffer, leaf extract catalyses the
204 conversion of H_2O_2 into H_2O and O_2 by oxidation of guaiacol, which was measured
205 spectrophotometrically at 436 nm.

206 *Syringaldazine peroxidase (SPx)* was determined in 80 mM Tris-HCl reaction buffer (pH 7.5)
207 [32]. Syringaldazine substrate (55 μM) was oxidised by SPx simultaneously with the
208 reduction of 1 mM H_2O_2 and was monitored at 530 nm.

209 *Glutathione-S-transferase (GST)* activity was determined using different standard substrates:
210 1 mM 1-chloro-2,4-dinitrobenzene (CDNB), 1 mM 1,2-dichloro-4-nitrobenzene (DCNB),
211 1 mM 4-nitrobenzyl chloride (NBC), 1 mM p-nitrobenzoyl chloride (NBoC), 0.5 mM p-
212 nitrophenylacetate (p-Npa) and fluorodifen (1.2 mM) [33,34]. By adding 1 mM glutathione
213 (GSH) to 1 mM of substrate in 75 mM KH_2PO_4 reaction buffer (pH 6.5), the formation of
214 conjugate was measured at respective wavelengths (340 nm, 345 nm, 310 nm, 310 nm,
215 400 nm and 400 nm).

216 *Ascorbate peroxidase (APx)* activity was determined after a separate extraction [35]. Plant
217 tissue (100 mg) was extracted using a modified extraction buffer, containing 0.1 M Tris-HCl
218 (pH 7.8), 1 mM DTT, 1 mM EDTA and 10 mM ascorbate. Ascorbate peroxidase reduces
219 H_2O_2 by oxidation of ascorbate (AsA) into dehydroascorbate (DHA). Adding 20 mM H_2O_2 to
220 the reaction buffer (0.1 M HEPES and 1 M EDTA, pH 7), made it possible to calculate APx
221 activity in leaf extract by monitoring the decrease of ascorbate (AsA) at 298 nm.

222

223 *Metabolite concentration and redox state*

224 Leaf tissue was extracted in 200 mM HCl. After centrifugation (16.000 g, 10 min, 4°C),
225 the supernatant was diluted with 200 mM NaH_2PO_4 (pH 5.6) and brought to pH 4.5 by
226 addition of 200 mM NaOH. This extract was used for determination of both AsA and GSH

227 concentrations and their redox state [36]. Eight biological replicates were used from each
228 condition. Ascorbate determination was based on ascorbate oxidase (AO) mediated oxidation
229 of AsA. Dithiotreitol (DTT, 25 mM) was added to one half of the leaf extract, reducing all
230 present DHA. By addition of AO to the subsample without DTT and the subsample with
231 DTT, the reduced fraction (AsA) and the total fraction of ascorbate (AsA & DHA) could be
232 determined by spectrophotometric measurement of the decrease in reduced ascorbate at
233 265 nm. Glutathione measurement was based on GSH mediated reduction of 5,5'-dithiobis-2-
234 nitrobenzoic acid (DTNB) that was analysed using a spectrophotometer at 412 nm. By
235 incubating half of the plant extract with 2-vinylpyridine for 30 minutes at 20°C, GSH was
236 inactivated and only the present oxidised fraction of glutathione (GSSG) could be measured.
237 By addition of GR to both incubated and non-incubated subsamples, GSSG and total GSH
238 concentration could be determined by monitoring the reduction of DTNB by GSH.

239

240 *Metazachlor determination in leaves*

241 Metazachlor was determined in aboveground biomass via reverse-phased high
242 performance liquid chromatography (RP-HPLC) (Adept CE-4200, Dual Piston Pump CE
243 4120, UV/VIS detector and Power Stream software, United Kingdom). For extraction, 5 g of
244 fresh plant tissue was homogenized in 5 mL pure acetonitrile (HPLC grade JTBaker ®). To
245 improve the recovery of polar components and to facilitate the partitioning of the solvent, 2 g
246 MgSO₄ was added to the extract. In order to reduce the amount of polar interferences 0.5 g
247 NaCl was added. By the addition of 0.5 g Na₃ Citrate x 2 H₂O and 0.25 g
248 Na₂H Citrate x 1.5 H₂O, the optimal pH of 6.5 was maintained. The extract was centrifuged
249 for 5 min at 1057 g at room temperature. One mL of supernatant was transferred to a
250 dispersive centrifuge tube (Spectrum ®, Chemical MFG Corp.) containing 25 mg of primary
251 secondary amine and 150 mg MgSO₄ and 2.5 mg of graphitised carbon black to remove

252 pigments. The tubes were mixed for 30 s and then centrifuged again for 5 min at 1057 g.
253 Subsequently, the collected supernatant was analysed by RP-HPLC. The samples were
254 analysed at 220 nm in a gradient regime by an analytical column Supelcosil LC-18 150 x
255 4.6 mm, 5 µm. The injected volume was 20 µL. The mobile phase composition was: phase A
256 acetonitrile: water (40:60) and phase B acetonitrile: water (80:20). The gradient was applied
257 for 20 min in the following regime; 0 min - 100 % A: 0 % B, 10 min - 50 % A: 50 % B,
258 20 min - 0 % A: 100 % B, with a flow rate of 1 mL/min. The limit of quantification and the
259 limit of detection of this analytical method contained 1.1 µg/mL and 0.4 µg/mL, respectively.
260 Quantification was based on a metazachlor standard curve prepared with certified
261 metazachlor standard (98.5 %, Dr Ehrenstorfer GmbH).

262

263 *Nutrient profile in leaves*

264 Dry leaf material (0.1-0.5 g) was digested in 70-71 % HNO₃ and dissolved in 2 % HCl.
265 After digestion, the clear colourless extract was brought to 25 mL volume with Milli-Q water.
266 Macronutrients (P, K, Mg, Ca, S) and micronutrients (Na, Fe, Cu, Zn, Mn) present in plant
267 extracts were determined by inductively coupled plasma – optical emission spectroscopy
268 (ICP-OES 710, Agilent Technologies, Australia). Concentrations were calculated by the use
269 of standard curves with known concentrations.

270

271 *Statistical analyses*

272 All data were processed according to one-way or 2-way ANOVA tests in open-source R
273 software (R 3.1.2, The R Foundation for Statistical Computing, Vienna, Austria), in strict
274 accordance to parametrical conditions. Normal distribution of the data was tested using
275 Shapiro-Wilk test. Following the ANOVA, post-hoc Tukey test was performed for multiple
276 pairwise comparisons. In case parametrical conditions were not met, Kruskal-Wallis,

277 followed by 2-by-2 Wilcoxon post-hoc comparison analyses were performed. Data are
278 represented as mean values \pm standard error (SE) and significance was set at 5 % level.
279

RESULTS

280
281
282
283
284
285
286
287
288
289
290
291
292
293
294
295
296
297
298
299
300
301
302
303
304

Growth, development and morphology of B. napus

Seven days after metazachlor application, seed germination was 10 % lower in microcosms treated with 0.2 and 0.4 mM metazachlor in comparison to the non-treated microcosms, although not significant (data not shown). Two weeks after treatment (14 DAT) 1.12 and 1.58 mg metazachlor /kg FW were found in the aerial parts of 0.2 and 0.4 mM metazachlor-treated plants, respectively. During the following 4 weeks, the levels of metazachlor decreased with 78 % and 64 % in the aerial plant parts of the respective treatments to 0.24 and 0.57 mg metazachlor /kg FW (42 DAT) (Figure 1). Closely after application leaves displayed fasciation in the form of crinkled leaves, shortened mid ribs and incomplete detachment of the leaves under the influence of metazachlor (Figure 2). These malformations appeared within the first 2 to 6 weeks after treatment and remained present until leaves' abscission during further development. Twenty-one DAT 20 % and 50 % of the plants treated with 0.2 and 0.4 mM metazachlor, respectively, displayed signs of fasciation and 20 % of the plants in both treatments did not survive the first 7 weeks (data not shown). Weight and height were strongly inhibited in 0.2 and 0.4 mM metazachlor-exposed plants at 14 DAT in a dose dependent way (Figure 3A, Figure 4 and Table 1). Twenty-eight DAT, these differences still existed (Figure 3B and Table 2), but at 63 DAT fresh weights of plants under different exposures were equal (Figure 3C). When taking a closer look into the rate of development of leaves of the young seedlings, no apparent differences were observed up to 5 weeks after metazachlor application (35 DAT) (Figure 5). However, considering leaf surface area and petiole length, the leaves appeared to be smaller under the influence of metazachlor, with smaller leaf surface area and shorter petioles which might explain the reduction in aboveground weight in the short term (Supplemental data S1). Between 5 and 7 weeks after application, metazachlor-exposed plants tended to develop leaves faster than control plants.

305 At 47 DAT, for example 30 % and 70 % of 0.2 and 0.4 mM metazachlor-exposed plants
306 respectively, were situated in growth stage 19 or 20, meaning that these plants had developed
307 9 or more leaves whereas all control plants had developed maximal 8 leaves (Figure 5).

308

309 *Enzymes and metabolites involved in detoxification*

310 The activity of GST significantly increased under the influence of metazachlor, at 14 and
311 28 DAT (Tables 1 and 2, **Figure 6**). The activity of GST was increased towards
312 chlorodinitrobenzene (CDNB), fluorodifen and nitrophenylacetate (Npa) substrates and not
313 found for 1,2-dichloro-4-nitrobenzene (DCNB), 4-nitrobenzyl chloride (NBC) and p-
314 nitrobenzpyl chloride (NBoC), with the strongest induction towards CDNB (Tables 1 and 2).
315 At both time points, the level of GSH, which is consumed during GST-catalysed
316 metabolism of xenobiotics such as herbicides, tended to be lower under the influence of
317 metazachlor (Figure 6). Whereas this trend could not be statistically underpinned, the redox
318 state of glutathione was significantly turned towards the oxidised form (GSSG) at 14 DAT
319 under influence of 0.4 mM metazachlor (Table 1). At 28 DAT, the redox state of GSH was
320 similar in all treatments.

321

322 *Metazachlor induces oxidative stress in the leaves of B. napus*

323 The presence of reactive oxygen species (ROS), *e.g.* H₂O₂, was visualised using 3,3'-
324 diaminobenzidine staining. No differences in the presence of H₂O₂ were detected at 14 DAT
325 since DAB staining was restricted to the veins in all conditions (Supplemental data S2). At 14
326 DAT, the total antioxidative capacity (TAC) in the leaves of *B. napus* tended to increase
327 under the influence of metazachlor, however this trend could not be statistically supported
328 (Table 1). At 28 DAT, a significant increase in the lipophilic fraction of antioxidants was
329 observed (Table 2). Additionally, the activities of enzymes involved in the antioxidative

330 defence (SOD, CAT, APx and GR) and cell wall lignification (GPx and SPx) were measured.
331 In general, the activities of all antioxidative enzymes increased with exposure to increasing
332 metazachlor doses (Tables 1 and 2). A higher activity in metazachlor-treated plants in
333 comparison to non-treated plants could be statistically confirmed for catalase (CAT),
334 ascorbate peroxidase (APx) and syringaldazine peroxidase (SPx) at 14 DAT and for
335 superoxide dismutase (SOD), catalase (CAT), glutathione reductase (GR) and guaiacol
336 peroxidase (GPx) at 28 DAT. Twenty-eight DAT, the levels of AsA were not affected by the
337 applied metazachlor treatments. Together with AsA, GSH is a key metabolite in the AsA-
338 GSH cycle, a supportive cycle behind the enzymatic antioxidative defence. The redox state of
339 GSH was significantly leaning towards the oxidised form (GSSG) under the influence of 0.4
340 mM metazachlor at 14 DAT.

341

342 *Metazachlor induces membrane lipid peroxidation and shifts in pigment and nutrient profiles*

343 The increasing trend in TBA-reactive metabolites of 39 % and 43 % in 0.2 mM and 0.4
344 mM metazachlor-exposed plants respectively, indicated that cellular membranes were
345 destabilised by lipid peroxidation at 28 DAT (Table 2). No clear shifts in pigment profile
346 were observed 2 weeks after application. Twenty-eight DAT however, the pigment profile in
347 *B. napus* leaves was influenced by 0.2 mM metazachlor with an increased chlorophyll
348 concentration, due to an increment of chlorophyll *a* (Table 2). Fourteen-day-old plants
349 exposed to 0.4 mM metazachlor contained higher nutrient levels in their aboveground areal
350 parts. Levels of macronutrients, such as potassium, calcium and phosphorus, as well as of
351 micronutrients, such as manganese and copper, increased significantly within a range of 25 to
352 80 % under the influence of 0.4 mM metazachlor (Table 1). Twenty-eight DAT, the nutrient
353 profile in metazachlor-treated plants differed from control plants, with significant losses of
354 phosphorus and significant augmentation of magnesium and sodium (Table 2).

355

356

DISCUSSION

357 In the present study, controlled growth experiments of oilseed rape were carried out using
358 microcosms in temperature-, light- and moisture-controlled growth chambers. This
359 experimental set-up enabled us to investigate the specific impact of metazachlor on the crop
360 *B. napus*, with exclusion of the complex interaction with soil characteristics and soil
361 organisms, the direction and rate of drainage and the presence of herbivores, such as snails.
362 Hence, the underlying mechanisms that ultimately determine the degree of phytotoxicity
363 could be studied.

364

365 *The detoxification metabolism in B. napus is activated 2 to 4 weeks after metazachlor*
366 *application*

367 The detoxification capacity of a crop is crucial for the neutralisation of xenobiotic
368 compounds and ultimately determines the potential harm induced by that compound, either in
369 form of direct interaction or via the induction of oxidative stress. The presence of metazachlor
370 in the aboveground organs of young oilseed seedlings pointed out that metazachlor was taken
371 up by roots and translocated into the shoots within 2 weeks after application. The decrease of
372 the internal metazachlor concentration in the aboveground parts of *B. napus* during the
373 subsequent weeks indicated the activation of the detoxification metabolism (Figure 1). The
374 rate of detoxification decreased with increasing metazachlor dose 2 weeks after application,
375 which might indicate that the detoxification metabolism is either suppressed by the high
376 internal metazachlor concentration or that it reached its maximal turnover (Figure 1). Taking
377 into account the rate of detoxification, the results of this laboratory test set up suggest that
378 metazachlor **might be entirely metabolised internally within 10 to 12 weeks after application**
379 (Figure 1). This result is in line with reported half-lives of metazachlor in the soil, that range

380 between 19 to 82 days [37]. In general, the detoxification rate of herbicides is determined by
381 the activity of cytochrome P450 peroxidases, GSH and GST. The detoxification of
382 chloroacetamides does not involve phase I metabolism by cyt P450 and is only facilitated
383 by GST-mediated conjugation [38]. However, the tolerance of a crop towards a certain
384 herbicide is not solely determined by the activity of GST. Glutathione concentration and
385 redox state are also important [10]. After metazachlor application, the increased activity of
386 GST at both time points and the increment in GSSG fraction at 14 DAT suggest that the
387 detoxification of metazachlor was activated in oilseed rape (Figure 6). Two weeks after
388 metazachlor application, the increased activity of GST with affinity towards CDNB and Npa
389 substrates indicates that metazachlor and its metabolites were being conjugated with GSH
390 prior to storage in the cell wall or in the vacuole (Figure 6). Four weeks after application,
391 GST showed affinity to all tested GST substrates (Figure 6). Phi class GST's are closely
392 associated with detoxification of chloroacetamides [17]. Since fluorodifen has been associated
393 with tau-class GST activity [39] and CDNB is considered as a non-specific substrate [11], it
394 can be considered that both tau and phi classes of GSTs, which are most important routes for
395 detoxification in plants [40], are involved in detoxification of metazachlor. Since the
396 glutathione redox state is promoted towards its oxidised form (GSSG) under metazachlor
397 treatment, GSH biosynthesis might not be able to provide the demand for GSH at this time
398 point (Table 1). Two weeks later, the augmented activity of GST indicates that glutathione is
399 still actively consumed for metazachlor-conjugation at this time point (Table 2, Figure 6). In
400 accordance with our results, the related chloroacetamide metolachlor induced a 5-fold
401 increase in GST activity in maize [41]. Although Viger et al. [41] did not observe any changes
402 in GSH content, Štajner et al. [20] noticed decreased GSH contents in lettuce, pea and bean
403 seeds under the influence of chloroacetamides, alachlor and metolachlor.

404

405 *Metazachlor-induced oxidative stress results in membrane damage of plant cells*

406 The presence of ROS, such as H₂O₂, in leaves of metazachlor exposed seedlings could not
407 be revealed with the 3,3'-diaminobenzidine staining technique. However, the increased
408 activity of enzymes involved in antioxidative defence and cell wall lignification and the
409 activation of the AsA-GSH cycle, indirectly suggest the induction of pro-oxidants under the
410 influence of metazachlor, 2 and 4 weeks after application (Tables 1 and 2, Figure 6). The total
411 antioxidative capacity in leaf cells, determined by the ferric reducing antioxidative capacity
412 (FRAP), comprises both water-soluble antioxidants, such as GSH, AsA, proline, phenolic
413 compounds, membrane-bound molecules, and water-insoluble antioxidants, such as
414 carotenoids and tocopherols (vitamin E) [42]. The increase of the lipophilic fraction of
415 antioxidants and the increase of carotenoid concentration at 28 DAT (Table 2), suggest a
416 potential role for tocopherols as antioxidative compounds at this time point. Tocopherols have
417 a significant role in herbicide-induced oxidative stress because of their ability to protect
418 membrane-localised polyunsaturated fatty acids against ROS-induced lipid peroxidation
419 [43,44]. However, the simultaneous increase in lipid peroxidation suggests insufficient
420 protection of leaf tissue against oxidative stress. Membrane integrity was estimated via
421 potassium leakage and lipid peroxidation. The latter was significantly induced by metazachlor
422 at 28 DAT (Table 2). Whereas the destabilisation of membranes can directly be induced
423 through the inhibition of fatty acid biosynthesis by metazachlor, this also can be the result of
424 metazachlor-induced oxidative stress. That these responses in membrane destabilisation
425 became significant after 4 weeks could either be explained by the fact that the inhibition of
426 VLCFA is a relatively slow process [23] or the fact that oxidative damage is a secondary side-
427 effect of metazachlor. In general, herbicide-induced oxidative stress has been described in
428 several crops [18,19] and in particular also for chloroacetamides, such as alachlor and
429 metolachlor [20,21]. The induction of the antioxidative enzymes SOD, APX, CAT and GR at

430 2 and 4 weeks after metazachlor application indicated metazachlor-induced oxidative stress
431 (Tables 1 and 2). The reduced CAT activity in the highest metazachlor treatment at 14 DAT
432 could be linked to the high phytotoxic effects of metazachlor. However, the high sensitivity of
433 CAT towards high levels of H₂O₂ has been described in different crop species under influence
434 of various stresses, such as copper [45], herbicides [46] and high and low temperatures [47].
435 The high activities of cell wall bound peroxidases that use syringaldazine and guaiacol as
436 substrates (Tables 1 and 2) and that are involved in lignin biosynthesis, suggest either the
437 apoplastic presence of ROS or the activation of cell wall lignification [48,49]. Increased cell
438 wall lignification could result in a reduced permeability by the establishment of a physical
439 barrier and can therefore allow the cell to better protect itself against xenobiotics. Lignin is
440 known to be responsive to a range of stresses. Biotic and abiotic stresses (such as metals), are
441 known to induce lignification in the walls of cells that do not lignify under non-stress
442 responses [50], however this has not been described yet for herbicides. The increased activity
443 of ascorbate peroxidase (APx) under the influence of 0.2 mM metazachlor at 14 DAT
444 indicates that H₂O₂ is being converted actively into water and oxygen (Figure 6) and suggests
445 the activation of the AsA-GSH cycle. This assumption is supported by the significant shift of
446 the glutathione redox state towards its oxidised form, glutathione disulphide (GSSG), at 14
447 DAT and the increased activity of GR at 28 DAT under the influence of metazachlor (Figure
448 6). Together with glutathione's shift towards its oxidised form, the increased activity of GST
449 implies that GSH is consumed in the detoxification metabolism of metazachlor. Therefore, it
450 can be presumed that GSH fulfils a dual role in both antioxidative defence and detoxification
451 (Figure 6). Although ROS are known to induce oxidative damage, they also have an important
452 function in signalling [51]. Hydrogen peroxide has been shown to regulate GST in vivo [52]
453 and can therefore influence the rate of detoxification. GST induction by ROS would appear to
454 represent an adaptive response as these enzymes detoxify some of the toxic carbonyl-,

455 peroxide-, and epoxide-containing metabolites produced within the cell by oxidative stress
456 [53].

457

458 *Metazachlor inhibits growth, induces fasciation and causes membrane peroxidation on the*
459 *short term*

460 Phytotoxic effects of metazachlor on oilseed rape became apparent shortly after its
461 application, with a reduction of germination (data not shown), the manifestation of fasciation
462 (Figure 2) and the occurrence of mortality (data not shown). Fasciation of the leaves was
463 already induced immediately after seedling emergence (Figure 2). Typical symptoms of
464 chloroacetamide herbicides, such as stunted growth, cupped and wrinkled leaves, shortened
465 main veins and leaf fasciation were induced and were formerly observed in *Arabidopsis*
466 *thaliana* exposed to related chloroacetamides, acetolachlor, alachlor and metolachlor [5].
467 Metazachlor-induced fasciation could be attributed to the mode of action of chloroacetamides,
468 whereby inhibition of VLCFA synthesis has led to the inhibition of normal cell division
469 [54,55]. During the further development of the crop, stem and shoot weight of the emerged
470 seedlings was suppressed by metazachlor (Figure 3A-C, Table 1 and 2). Reductions in crop
471 shoot length have previously been observed in *Sorghum sp.* under the influence of the
472 chloroacetamide, metolachlor [56]. Although the timing of appearance of the leaves of *B.*
473 *napus* seedlings seemed not to be influenced by metazachlor (Figure 5), the surface of the
474 leaves and the petiole length were noticeably reduced (Supplemental data S1) and could be
475 linked with an insufficient capacity of light capitation for photosynthesis and therefore
476 reduced shoot weight. However, the pigment profile was not influenced as such (Tables 1 and
477 2). In contrast to previous studies where pigment content was negatively affected by
478 pesticides [8,57], chlorophyll and carotenoid concentrations rather tended to increase under
479 the influence of metazachlor (Tables 1 and 2). Although, metazachlor did not have any effect

480 on the rate of leaf development up to 5 weeks after treatment, metazachlor-exposed plants
481 tended to develop leaves faster than control plants between 5 and 7 weeks after treatment
482 (Figure 5). Taking into consideration the development of leaves and the similar weights of
483 metazachlor exposed and non-exposed seedlings 9 weeks after application (Figure 3C), the
484 seedlings appeared to recover from the initial herbicide stress by investing in leaf
485 development.

486

487 *Conclusions*

488 In conclusion, this controlled microcosm experiment demonstrated that, on the short term,
489 metazachlor induces significant adverse effects on oilseed rape at morphological level.
490 Together with an induction of the detoxification metabolism and the activation of the
491 antioxidative defence responses, a reduction in growth investment was observed. These
492 observations underpin the hypothesis that plants are investing energy in detoxification of the
493 absorbed metazachlor and in the neutralisation of metazachlor-induced ROS, over shoot
494 growth. This strategy seems to suffice for the plants to recover, as 9 weeks after application
495 their weight did not differ any more from the non-treated plants. When considering the weight
496 of the aboveground areal plant parts, the metazachlor-exposed plants appear to be able to
497 recover from the initial chemical-induced stress.

498

ACKNOWLEDGEMENT

499 We thank A. Wijgaerts and C. Put for their technical assistance of the microcosm
500 experiment. The present study was supported by a PhD grant for Hanne Vercampt from the
501 Institute for the Promotion of Innovation through Science and Technology in Flanders (IWT-
502 Vlaanderen). We especially thank G. Chotoklieva for the technical assistance of the
503 metazachlor analyses.

504

REFERENCES

- 505 1. Fuerst EP. 1987. Understanding the mode of action of the chloroacetamide and
506 thiocarbamate herbicides. *Weed Technol.* 1:270–277.
- 507 2. Mamy L, Barriuso E, Gabrielle B. 2005. Environmental fate of herbicides trifluralin,
508 metazachlor, metamitron and sulcotrione compared with that of glyphosate, a substitute
509 broad spectrum herbicide for different glyphosate-resistant crops. *Pest Manag. Sci.*
510 61:905–916.
- 511 3. Carpenter D, Boutin C. 2010. Sublethal effects of the herbicide glufosinate ammonium
512 on crops and wild plants: Short-term effects compared to vegetative recovery and plant
513 reproduction. *Ecotoxicology.* 19:1322–1336.
- 514 4. Foy CL, Witt HL. 1990. Seed Protectants Safen Sorghum (*Sorghum bicolor*) Against
515 Chloroacetamide Herbicide Injury. 4:886–891.
- 516 5. DeRidder BP, Goldsbrough PB. 2006. Organ-specific expression of glutathione S-
517 transferases and the efficacy of herbicide safeners in *Arabidopsis*. *Plant Physiol.*
518 140:167–175.
- 519 6. Cui J, Zhang R, Wu GL, Zhu HM, Yang H. 2010. Salicylic acid reduces Napropamide
520 toxicity by preventing its accumulation in rapeseed (*Brassica napus* L.). *Arch. Environ.*
521 *Contam. Toxicol.* 59:100–108.
- 522 7. Jiang L, Ma L, Sui Y, Han SQ, Wu ZY, Feng YX, Yang H. 2010. Effect of manure
523 compost on the herbicide prometryne bioavailability to wheat plants. *J. Hazard. Mater.*
524 184:337–344.
- 525 8. Xiao LY, Jiang L, Ning HS, Yang H. 2008. Toxic reactivity of wheat (*Triticum*
526 *aestivum*) plants to herbicide isoproturon. *J. Agric. Food Chem.* 56:4825–4831.

- 527 9. Jablonkai I, Biology M, Stress P, Pathology P, Science W, April R, Sc A, Sc A, Gst S,
528 Gstcacetofhlor R, Re- P. 1991. Role of Glutathione and Glutathione S-Transferase in
529 the Selectivity of Acetochlor in Maize and Wheat. 231:221–231.
- 530 10. Hatton PJ, Dixon D, Coleb DJ, Edwardsa R. 1996. Glutathione Transferase Activities
531 and Herbicide Selectivity in Maize and Associated Weed Species. *Pestici. Sci.*
532 doi:10.1002/(SICI)1096-9063(199603)46:3<267::AID-PS347>3.0.CO;2-N.
- 533 11. Cole DJ. 1994. Detoxification and activation of agrochemicals in plants. *Pestic. Sci.*
534 42:209–222.
- 535 12. Scarponi L, Quagliarini E, Del Buono D. 2006. Induction of wheat and maize
536 glutathione S-transferase by some herbicide safeners and their effect on enzyme
537 activity against butachlor and terbuthylazine. *Pest Manag. Sci.* 62:927–932.
- 538 13. Dixon DP, Edwards R. 2010. Glutathione Transferases. *Arab. B.*, pp 1–15. doi:e0131.
539 10.1199/tab.0131.
- 540 14. Dixon DP, Cummins I, Cole DJ, Edwards R. 1998. Glutathione-mediated
541 detoxification systems in plants. *Curr. Opin. Plant Biol.* 1:258:266.
- 542 15. Edwards R, Dixon DP, Walbot V. 2000. Plant glutathione S -transferases: enzymes
543 with multiple functions in sickness and in health. 5:193–198.
- 544 16. Marrs K a. 1996. the Functions and Regulation of Glutathione S-Transferases in Plants.
545 *Annu. Rev. Plant Physiol. Plant Mol. Biol.* 47:127–158.
- 546 17. Cho HY, Yoo SY, Kong KH. 2006. Cloning of a rice tau class GST isozyme and
547 characterization of its substrate specificity. *Pestic. Biochem. Physiol.* 86:110–115.
- 548 18. Gill SS, Tuteja N. 2010. Reactive oxygen species and antioxidant machinery in abiotic
549 stress tolerance in crop plants. *Plant Physiol. Biochem.* 48:909–930.

- 550 19. Faheed FA. 2012. Comparative effects of four herbicides on physiological aspects in
551 *Triticum sativum* L. *Afr. J. Ecol.* 50:29–42.
- 552 20. Štajner D, Popović M, Štajner M. 2003. Herbicide induced oxidative stress in lettuce,
553 beans, pea seeds and leaves. *Biol. Plant.* 47:575–579.
- 554 21. Liu HJ, Xiong MY, Tian BL. 2012. Comparative phytotoxicity of Rac-metolachlor and
555 S-metolachlor on rice seedlings. *J. Environ. Sci. Heal. Part B.* 47:410–419.
- 556 22. Dean J V, Gronwald JW, Eberlein C V. 1990. Induction of glutathione s-transferase
557 isozymes in sorghum by herbicide antidotes. *Plant Physiol.* 92:467–73.
- 558 23. Dayan FE, Watson SB. 2011. Plant cell membrane as a marker for light-dependent and
559 light-independent herbicide mechanisms of action. *Pestic. Biochem. Physiol.* 101:182–
560 190.
- 561 24. Kopsell D a., Armel GR, Abney KR, Vargas JJ, Brosnan JT, Kopsell DE. 2011. Leaf
562 tissue pigments and chlorophyll fluorescence parameters vary among sweet corn
563 genotypes of differential herbicide sensitivity. *Pestic. Biochem. Physiol.* 99:194–199.
- 564 25. Lancashire PD, Bleiholder H, Boom T Van Den, LangelÜDdeke P, Stauss R, Weber E,
565 Witzemberger a. 1991. A uniform decimal code for growth stages of crops and weeds.
566 *Ann. Appl. Biol.* 119:561–601.
- 567 26. Dhindsa R, Plumbdhinsa P, Thorpe T. 1981. Leaf senescence: correlated with
568 increased levels of membrane permeability and lipid peroxidation, and decreased levels
569 of superoxide dismutase. *J. Exp. Bot.* 32:93–101.
- 570 27. Lichtenthaler HK, Buschmann C, Knapp M. 2005. How to correctly determine the
571 different chlorophyll fluorescence parameters and the chlorophyll fluorescence
572 decrease ratio RFd of leaves with the PAM fluorometer. *Photosynthetica.* 43:379–393.

- 573 28. Daudi A, Cheng Z, O'Brien JA, Mammarella N, Khan S, Ausubel FM, Bolwell GP.
574 2012. The Apoplastic Oxidative Burst Peroxidase in *Arabidopsis* Is a Major
575 Component of Pattern-Triggered Immunity. *Plant Cell*. 24:275–287.
- 576 29. Kerchev P, Ivanov S. 2008. Influence of extraction techniques and solvents on the
577 antioxidant capacity of plant material. *Biotechnol. Biotechnol. Equip.* 22:556–559.
- 578 30. McCord JM, Fridovich I. 1969. Superoxide dismutase: an enzymatic function for
579 erythrocyte hemoglobin. *J. Biol. Chem.*:6049–6055.
- 580 31. Bergmeyer HU, Gawenn K, Grassl M. 1974. Enzymes as biochemical reagents.
581 *Methods Enzym. Anal.*, pp 425–522.
- 582 32. Czaninski Y, Imberty A, Catesson A. 1984. Cytochemical-localization and parallel
583 biochemical analysis of vegetal peroxidases. *Biol. Cell*. 51:A34–A34.
- 584 33. Schröder P, Collins C. 2002. Conjugating Enzymes Involved in Xenobiotic
585 Metabolism of Organic Xenobiotics in Plants. *Int. J. Phytoremediation*. 4:247–265.
- 586 34. Scalla R, Roulet A. 2002. Cloning and characterization of a glutathione S-transferase
587 induced by a herbicide safener in barley (*Hordeum vulgare*). *Physiol. Plant*. 116:336–
588 344.
- 589 35. Gerbling K, Kelly G, Fischer K, Latzko E. 1984. Partial purification and properties of
590 soluble ascorbate peroxidases from pea leaves. *J. Plant Physiol*. 115:59–67.
- 591 36. Queval G, Noctor G. 2007. A plate reader method for the measurement of NAD,
592 NADP, glutathione, and ascorbate in tissue extracts: Application to redox profiling
593 during *Arabidopsis* rosette development. *Anal. Biochem*. 363:58–69.
- 594 37. Mamy L, Gabrielle B, Barriuso E. 2008. Measurement and modelling of glyphosate
595 fate compared with that of herbicides replaced as a result of the introduction of

- 596 glyphosate-resistant oilseed rape. *Pest Manag. Sci.*:262–275. doi:10.1002/ps.1519.
- 597 38. Coleman JOD, Randall R, Blake-Kalff MMA. 1997. Detoxification of xenobiotics in
598 plant cells by glutathione conjugation and vacuolar compartmentalization: A
599 fluorescent assay using monochlorobimane. *Plant, Cell Environ.* 20:449–460.
- 600 39. Jo HJ, Lee JJ, Kong KH. 2011. A plant-specific tau class glutathione S-transferase
601 from *Oryza sativa* with very high activity against 1-chloro-2,4-dinitrobenzene and
602 chloroacetanilide herbicides. *Pestic. Biochem. Physiol.* 101:265–269.
- 603 40. Thom R, Cummins I, Dixon DP, Edwards R, Cole DJ, Laphorn AJ. 2002. Structure of
604 a tau class glutathione S-transferase from wheat active in herbicide detoxification.
605 *Biochemistry.* 41:7008–7020.
- 606 41. Viger PR, Eberlein C V, Fuerst EP, Gronwald JW. 1991. Effects of CGA-154281 and
607 temperature on metolachlor absorption and metabolism , glutathione content , and
608 glutathione-s-transferase activity in corn. *Weed Sci.* 39:324–328.
- 609 42. Prior R, Wu X, Schaich K. 2005. Standarized Methods for the Determination of
610 Antioxidant Capacity and Phenolics in Foods and Dietary Supplements. *J. Agric. Food*
611 *Chem.* 53:4290–4302.
- 612 43. Fryer MJ. 1992. The antioxidant effects of thylakoid Vitamin E (alpha-tocopherol).
613 *Plant, Cell Environ.* 15:381–392.
- 614 44. Munné-Bosch S. 2005. The role of α -tocopherol in plant stress tolerance. *J. Plant*
615 *Physiol.* 162:743–748.
- 616 45. Luna CM, Gonzalez CA, Trippi VS. 1994. Oxidative damage caused by an excess of
617 copper in Oat leaves. *Plant Cell Physiol.*:11–15.
- 618 46. Song NH, Yin X Le, Chen GF, Yang H. 2007. Biological responses of wheat (*Triticum*

- 619 aestivum) plants to the herbicide chlorotoluron in soils. *Chemosphere*. 68:1779–1787.
- 620 47. Feierabend J, Schaan C, Hertwig B. 1992. Photoinactivation of Catalase Occurs under
621 Both High- and Low-Temperature Stress Conditions and Accompanies Photoinhibition
622 of Photosystem II. *Plant Physiol*. 100:1554–1561.
- 623 48. Bestwick CS. 1998. Localized Changes in Peroxidase Activity Accompany Hydrogen
624 Peroxide Generation during the Development of a Nonhost Hypersensitive Reaction in
625 Lettuce. *Plant Physiol*. 118:1067–1078.
- 626 49. Lee BR, Kim KY, Jung WJ, Avice JC, Ourry A, Kim TH. 2007. Peroxidases and
627 lignification in relation to the intensity of water-deficit stress in white clover (*Trifolium*
628 *repens* L.). *J. Exp. Bot*. 58:1271–1279.
- 629 50. Wang S, Li H, Lin C. 2013. Physiological, biochemical and growth responses of Italian
630 ryegrass to butachlor exposure. *Pestic. Biochem. Physiol*. 106:21–27.
- 631 51. Mittler R, Vanderauwera S, Gollery M, Van Breusegem F. 2004. Reactive oxygen gene
632 network of plants. *Trends Plant Sci*. 9:490–498.
- 633 52. Levine A, Tenhaken R, Dixon R, Lamb C. 1994. H₂O₂ from the oxidative burst
634 orchestrates the plant hypersensitive disease resistance response. *Cell*. 79:583–593.
- 635 53. Hayes JD, Pulford DJ. 1995. The Glutathione S-Transferase Supergene Family:
636 Regulation of GST* and the Contribution of the Isoenzymes to Cancer
637 Chemoprotection and Drug Resistance. *Crit. Rev. Biochem. Mol. Biol*. 30:445–600.
- 638 54. Böger P, Matthes B, Schmalfuß J. 2000. Towards the primary target of
639 chloroacetamides –new findings pave the way. *Pest Manag. Sci*. 56:497–508.
- 640 55. Wu J, Hwang I-T, Hatzios KK. 2000. Effects of Chloroacetanilide Herbicides on
641 Membrane Fatty Acid Desaturation and Lipid Composition in Rice, Maize, and

- 642 Sorghum,. *Pestic. Biochem. Physiol.* 66:161–169.
- 643 56. Wilkinson RE, Duncan RR, Meredith SA, Hatzios KK. 1993. Growth and
644 physiological responses of sorghum cultivars exposed to excess H⁺ and the herbicide
645 metolachlor. *Can. J. Bot.*:533–540.
- 646 57. Serra AA, Couée I, Renault D, Gouesbet G, Sulmon C. 2015. Metabolic profiling of
647 *Lolium perenne* shows functional integration of metabolic responses to diverse
648 subtoxic conditions of chemical stress. *J. Exp. Bot.* 66:1801–1816.
- 649

650

FIGURE LEGENDS

651 **Figure 1.** Metazachlor concentration in aboveground plant parts of *B. napus* 14, 28 and 42
652 DAT with 0 mM, 0.2 mM and 0.4 mM metazachlor. Data are presented as average values of
653 minimal 3 biological replicates \pm SE.

654

655 **Figure 2.** Detailed images of *B. napus* exposed to 0 mM, 0.2 mM and 0.4 mM metazachlor at
656 21 DAT. Plants exposed to 0.2 mM and 0.4 mM metazachlor displayed malformations of the
657 leaves.

658

659 **Figure 3.** Aboveground fresh weight of *B. napus* 14 DAT (A), 28 DAT (B) and 63 DAT (C)
660 with 0 mM, 0.2 mM and 0.4 mM metazachlor. Data are presented as average values of
661 minimal 10 biological replicates \pm SE. (*post-hoc values: $p < 0.05$)

662

663 **Figure 3.** Overview images of *B. napus* exposed to 0 mM, 0.2 mM and 0.4 mM metazachlor
664 at 14, 28 and 42 DAT.

665

666 **Figure 4.** Emergence and leaf development of *B. napus* over time, treated with (A) 0 mM, (B)
667 0.2 mM and (C) 0.4 mM metazachlor, expressed as the amount (%) of all measured plants
668 that are situated in a specific developmental stage at a certain time point (DAT). Different
669 growth stages are depicted as described by Lancashire et al. 1991.

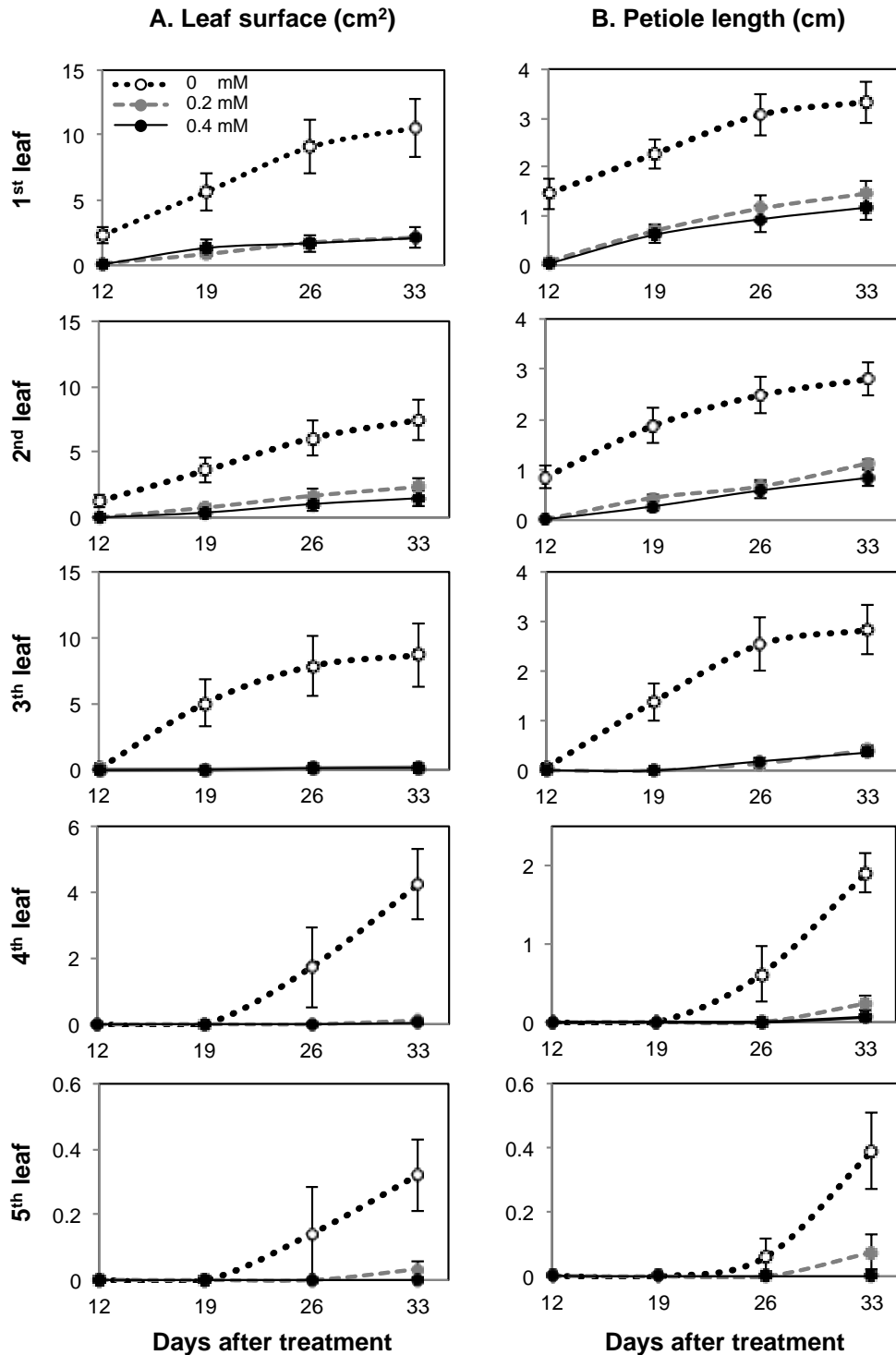
670

671 **Figure 5:** An overview of the relative enzyme activities and metabolite concentrations that
672 play a role in either the detoxification of herbicides or the antioxidant defence mechanism.
673 Data are expressed relative to control values (dashed line). Abbreviations used: APx

674 (ascorbate peroxidase), AsA (ascorbate), CDNB (chlorodinitrobenzene), GST (glutathione-S-
675 transferase), DHA (dehydroascorbate), GSSG (glutathione disulphide), GSH (glutathione),
676 GR (glutathione reductase), Npa (nitrophenylacetate), NADPH (Nicotinamide adenine
677 dinucleotide phosphate). (* post-hoc value $p < 0.05$)

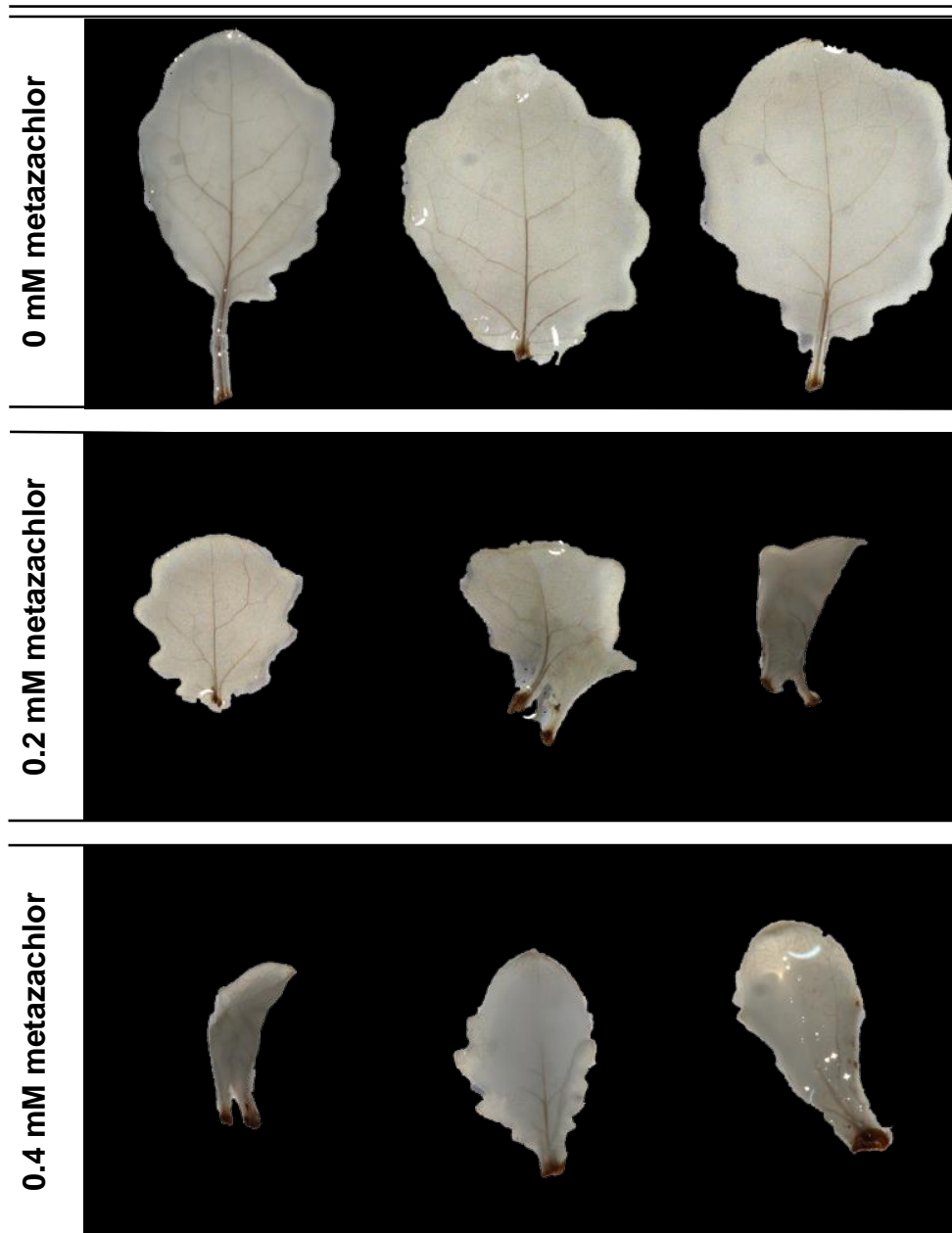
SUPPLEMENTAL DATA

679 **Supplemental data S1.** Leaf development of *B. napus* monitored weekly, after pre-emergent
 680 application with 0 mM (dotted line), 0.2 mM (dashed line) and 0.4 mM (solid line)
 681 metazachlor. Leaf surface (A) area and petiole length (B) were measured at 12, 19, 26 and 33
 682 DAT.



684 **Supplemental data S2.** Qualitative determination of H₂O₂ in leaves of *B. napus*, 14 days
685 after metazachlor application (0 mM, 0.2 mM, 0.4 mM) by 3,3'-diaminobenzidine staining.
686 Three biological replicates are shown per treatment.

14 Days after treatment



687